Development of polysilazane-based coatings embedding AgNPs-decorated silica nanospheres for further antimicrobial applications

Ceramics International 51 (2025) 66085–66094

Contents lists available at ScienceDirect

Ceramics International

journal homepage: www.elsevier.com/locate/ceramint

Development of polysilazane-based coatings embedding AgNPs-decorated silica nanospheres for further antimicrobial applications

Francesca Gattucci, Marta Miola, Cristina Balagna *

Department of Applied Science and Technology, Politecnico di Torino, Corso Duca degli Abruzzi 24, 10129, Turin, Italy

ARTICLE INFO

Keywords:
Composite coating
Polysilazane
Silica nanospheres
Silver nanoparticles

ABSTRACT

Amid global concerns regarding the proliferation of superbugs and viruses, new antimicrobial coatings have been explored to devise innovative solutions. In this context, this work presents a novel approach not previously reported in the literature, involving the synthesis of a composite coating composed of a polymeric ceramic precursor and silica nanoparticles decorated with silver nanoparticles. These nanoparticles are produced through a sol-gel synthesis process; subsequently, they are incorporated into a polymeric matrix to introduce silver as the antibacterial agent. The resulting coating is manually applied onto soda lime substrates.

The characterization process unfolds in two phases. Firstly, the silver-decorated silica nanospheres undergo examination via field-emission scanning electron microscopy, energy-dispersive X-ray spectroscopy, and X-ray diffraction analysis to confirm the synthesis of silver nanoparticles onto silica nanospheres and to evaluate their morphology, structure, and concentration. The antibacterial effectiveness of the synthesized filler is then demonstrated through a zone of inhibition test using *Staphylococcus epidermidis*. Subsequently, the coating, comprising a polysilazane as a ceramic precursor (commercially known as Durazane 1800) and the filler, was characterized in the same way, evaluating its morphology, composition, and structure. Additionally, the antibacterial efficacy is verified by means of the zone of inhibition test.

After incorporation into the polymeric matrix, the resulting composite coatings were homogeneous and dense. Structural characterization by X-ray diffraction confirmed the presence of metallic silver in the coatings, while scanning electron microscopy showed that the nanospheres were evenly dispersed within the polysilazane matrix but mostly encapsulated. Antibacterial tests on the coatings did not show an inhibition zone, likely due to the limited exposure of the silver nanoparticles caused by the dense and non-porous nature of the matrix. These findings highlight the importance of optimizing matrix porosity and surface accessibility in future studies to enhance the antibacterial performance of such hybrid coatings.

1. Introduction

Microbial contamination of some commonly used surfaces, such as medical devices, food packaging, high-touch public objects, textiles and air filtration systems, represents a significant global concern, as it can compromise the functionality, safety and durability of these materials [1]. Moreover, it contributes to the global challenge of antimicrobial resistance (AMR) [2]. In fact, in the European Union (EU), AMR results in approximately 33,000 deaths annually and incurs healthcare expenses and productivity losses amounting to EUR 1.5 billion per year [3]. The misuse or overuse of conventional antimicrobials in humans or animals significantly contributes to the proliferation of AMR [4] underscoring the need to prevent bacterial contamination [5].

The antimicrobial properties of silver, particularly in nanoparticle form, are well-documented and recognized [6]. The antibacterial mechanism of silver nanoparticles (AgNPs) is not completely discovered but it could be ascribable to two main effects: the release of Ag ions and the innate reactivity of nanoparticles. AgNPs penetrate the bacterial cell membranes, causing cell death and, in the meanwhile, silver ions, absorbed by the cell, disrupt ATP production and DNA replication, also generating reactive oxygen species (ROS), which further help in killing bacteria [7]. Even though the antiviral mechanism of action is not clear, silver nanoparticles have also shown an effective power against viruses including SARS-CoV-2 [8] and a wide range of other viruses, by inactivating or morphologically altering the infectious viral particles or by inhibiting the viral replication [9].

* Corresponding author.
E-mail address: cristina.balagna@polito.it (C. Balagna).

https://doi.org/10.1016/j.ceramint.2025.11.298
Received 2 September 2025; Received in revised form 5 November 2025; Accepted 21 November 2025
Available online 21 November 2025

In order to maximize the benefits associated with the use of AgNPs simultaneously reducing the risks related to their cytotoxicity, release and accumulation, processes able to embed them in matrixes and coatings are often utilized. Composite coatings containing silver nanoparticles are useful as they allow to the protection of the nanoparticles from the external environment (and vice versa), minimizing corrosion and oxidation phenomena, the unintentional dispersion of them in the surrounding environment and increasing the duration and control of the antimicrobial effect over time [10,11]. Several materials have been used as matrix for incorporating silver nanoparticles including glasses [11, 12], ceramics [13,14] and polymers [15,16]. Many antimicrobial polymer matrix composites have been synthesized through the introduction of antibacterial agents such as silver, copper or zinc oxide nanoparticles [17–19].

Polysilazanes are a fascinating class of polymers characterized by Si-N bonds in their backbones and pendent carbon-containing groups [20]. They are extensively used in coating applications due to the outstanding thermal and mechanical properties of the resulting products [21]. Notably, polysilazanes can act as ceramic precursors in the polymer-derived-ceramics (PDC) technique. Pyrolyzing inorganic polymers at relatively low temperatures presents an interesting method for producing ceramics. This approach serves as an alternative for creating ceramic coatings and fibers, compared to traditional sintering methods [22]. Incorporating AgNPs in a polysilazane matrix is a first step to obtain composite ceramic coatings at lower temperatures, without wasting material and with inexpensive deposition techniques [23] while combining the inherent antibacterial activity of silver nanoparticles with the advantageous properties of polysilazanes. Their excellent adhesion to substrates and high-density result in high-performance coatings [24]. Leveraging these attributes, polysilazanes have already been employed in various functional coatings, including anti-corrosive, anti-graffiti and anti-adherent systems [25]. Although some studies have explored the integration of silver species in polysilazane-derived ceramic coatings for antibacterial purposes, such as the work by *Bakumov* et al., which demonstrated the effectiveness of silver-loaded polysilazane matrices [22], the overall literature on the topic remains limited. In particular, dispersing AgNPs in an organic phase is challenging [26] and metal nanoparticles often tend to aggregate. Dispersing nanoparticles as dopants in silica materials and use them as a filler in the polysilazane matrix is an effective solution to prevent the aggregation during all the steps of the process (preparation, application and storage) [27]. In fact, combining AgNPs with a material that act as a carrier can improve the stability and dispersibility of AgNPs. In particular, silica nanospheres are suitable for this application thanks to their stability [28] and their compatibility with polysilazane polymers [29]. In the PDC technique, second phases or fillers like silica (SiO_2) [30] and zirconia (ZrO_2) powders are frequently used as passive fillers [31] to mitigate the substantial volume shrinkage that can result in defects, cracks or even delamination of the coatings [32]. The incorporation of fillers not only aids in addressing shrinkage issues but also facilitates the development of coatings with enhanced functionalities such as distinctive friction properties, electrical or thermal conductivity and catalytic activity [33].

Silica nanospheres ($nSiO_2$) have found extensive application as fillers in various composite materials, including silica-epoxy composites [34], coatings [35] and in reinforced acrylic coatings [36].

Hybrid materials combining silica nanostructures with functional components such as silver nanoparticles have gained increasing interest, as the $nSiO_2$ can serve as a carrier that prevents nanoparticle aggregation during synthesis, processing, and storage [27].

Among the different types of silica materials, mesoporous silica has also attracted significant attention as a host for silver species, both ions [37] and nanoparticles [38,39], due to its large surface area and tunable porosity, which facilitate both nanoparticle loading and controlled silver ion release.

Numerous studies detail methods for silver introduction into silica nanostructures in order to obtain strong antimicrobial agents [40,41]. However, the sol-gel process is the most common employed for the synthesis of silica nanospheres ($nSiO_2$) [42], with protocols adaptable for the incorporation of other elements onto the $nSiO_2$, like biotin, palladium, gold [43–45] and, also, silver [46,47]. The Stöber method is a widely used sol-gel approach for synthesizing $nSiO_2$. Its high degree of control over growth and reaction kinetics enable the creation of numerous varieties of silica particles that have been produced since its development [48]. Moreover, it is possible to easily functionalize Stöber-synthesized $nSiO_2$ for example by introducing ionic compounds onto $nSiO_2$ surface like in the synthesis of bioactive glass nanoparticles [49] or for synthesizing AgNPs decorated SiO_2 nanospheres, reducing the ionic form in the metallic state via heat treatment at 600 °C for 2 h [50].

The aim of this work is the development of AgNPs-decorated SiO_2 nanospheres (AgNPs-$nSiO_2$) to be incorporated in a polysilazane matrix in order to obtain a composite material for potential antimicrobial purposes. The process could be divided into two steps, starting from the synthesis and characterization of the AgNPs-decorated SiO_2 nanospheres (AgNPs-$nSiO_2$), followed by their dispersion into the matrix to assess compatibility with the polysilazane, with variations in the metal concentration. This composite approach not only enables the introduction of antibacterial functionality but also benefits from the intrinsic properties of polysilazane-derived coatings, such as mechanical strength, thermal resistance, and antiadhesive behavior, making the material potentially suitable for multifunctional applications in areas like medical devices and food contact surfaces.

2. Materials and methods

2.1. Materials

Tetraethyl orthosilicate (TEOS, at 99 % Sigma Aldrich), ethyl alcohol (EtOH, 99,5 %, Sigma Aldrich), 33 % ammonium hydroxide (NH_4OH, Sigma Aldrich) and Milli-Q water (H_2O) were used in the sol-gel synthesis of silica nanospheres. Silver nitrate ($AgNO_3$, 99 %, Sigma Aldrich) was used as the precursor for metallic silver nanoparticles. Polysilazane Durazane 1800 (Merck) served as the polymeric ceramic precursor for obtaining the matrix for the coating.

2.2. Synthesis of AgNPs-$nSiO_2$

The synthesis of AgNPs decorated SiO_2 nanospheres (AgNPs-$nSiO_2$) was adapted from a previously established protocol developed by *Miola* et al. for producing spherical monodispersed bioactive glass nanoparticles co-doped with boron and copper [51]. The synthesis process is reported in Fig. 1. The first step involved the preparation of two solutions, one composed of 93 mL of ethanol and 11,2 mL of tetraethyl orthosilicate and the second composed of 46 mL of Milli-Q water, 30 mL of ethanol and 17 mL of ammonium hydroxide, separately mixed for 30 min. Subsequently, these solutions were combined and stirred for an additional 30 min to initiate the synthesis of silica nanospheres ($nSiO_2$). Two approaches were followed at this point. The resulting solution was divided into two parts (solution A and solution B) to obtain two different concentrations of silver. Solution An underwent a first centrifugation at 7000 rpm for 5 min to remove excess supernatant before the addition of silver precursor, to test the influence of the amount of solvent on the resulting silver content. After the removal of the solvent, silver nitrate was added (0.743 g) followed by stirring for 1 h. In contrast, silver nitrate was directly introduced into solution B in the same quantity of solution A and left to stir for the same amount of time. Both solutions were then centrifuged again at 7000 rpm for 5 min and dried for 24 h at 60 °C. The resulting powders underwent heat treatment at 700 °C for 2 h with a ramp rate of 5 °C/min. The two Ag-doped powders were labeled as follows: *AgNPs-$nSiO_2$ A* for the nanospheres subjected to double centrifugation from solution A, and *AgNPs-$nSiO_2$ B* for those subjected to

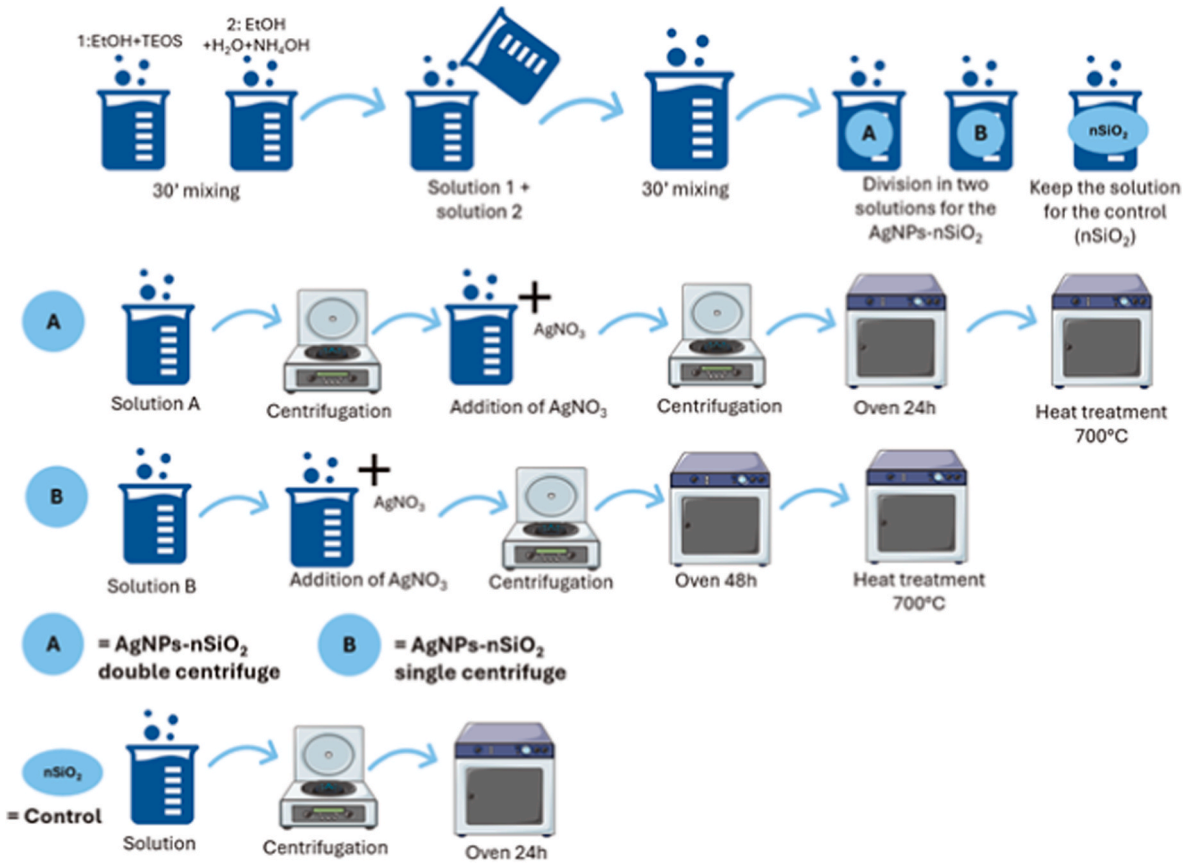

Fig. 1. Scheme of the synthesis of AgNPs-$nSiO_2$ –A and AgNPs-$nSiO_2$ - B. The picture was drawn partially using images from Servier Medical Art. Servier Medical Art by Servier is licensed under a Creative Commons Attribution 3.0 Unported License (https://creativecommons.org/licenses/by/3.0/).

single centrifugation from solution B. After the heat treatment, approximately 1 g of AgNPs–$nSiO_2$ powder was obtained for each synthesis route. Undoped $nSiO_2$ powders were also produced as control without adding $AgNO_3$.

2.3. Synthesis of the composite coating Dur-$nSiO_2$-AgNPs

The powders obtained from the heat treatment were then manually mixed to the Durazane 1800 polymer in a 33 wt% concentration. The mixture was manually deposited with a 100 μm film applicator onto sodalime substrates and left to dry under fume hood for 48h. Two samples were obtained and later characterized: the coating obtained from Durazane 1800 and AgNPs-$nSiO_2$-A was labeled *Dur-AgNPs-$nSiO_2$ A* and the coating obtained from Durazane 1800 and AgNPs-$nSiO_2$-B was labeled *Dur-AgNPs-$nSiO_2$ B*. The coating manually mixing only Durazane polymer and $nSiO_2$ without silver (*Dur-$nSiO_2$*) was prepared as control and manually deposited on the sodalime substrates. To ensure reproducibility, the synthesis of AgNPs-decorated silica nanospheres and the preparation of the composite coatings were repeated multiple times.

2.4. Physical - chemical analysis

Both the powders, AgNPs-$nSiO_2$-A and -B and the relative coatings, Dur-AgNPs-$nSiO_2$-A and -B were analyzed through field-emission electron microscopy equipped with Energy Dispersive X-ray Spectrometry (FESEM-EDS SUPRATM 40, Zeiss and Merlin Gemini Zeiss and MIRA3 XMH, TESCAN) in order to observe morphology in top view and cross section and composition. The FESEM images of the powders were subsequently processed using ImageJ software to determine the average size of the silica nanospheres and the silver nanoparticles, based on 20 individual measurements. X-ray diffractometry (XRD, Bragg–Brentano X'pert Philips diffractometer) was used to investigate the crystalline structure of the obtained products. The patterns obtained from AgNPs-$nSiO_2$ powders were compared to those from $nSiO_2$ powders produced using the Stöber method without AgNPs functionalization. The average crystallite size of the AgNPs on the $nSiO_2$ surface was estimated from the most intense diffraction peak using the Scherrer equation. Similarly, the XRD patterns for the coatings were compared, using a Dur-$nSiO_2$ coating made with Durazane 1800 and undecorated silica nanospheres. In addition, Attenuated Total Reflectance Fourier-Transform Infrared spectroscopy (ATR-FTIR, Nicolet iS 50 Spectrometer (Thermo Scientific, Milan, Italy)) was utilized to characterize the chemical composition of the filler and the composite coatings.

2.5. Antibacterial test

The antibacterial efficacy of the powders AgNPs-$nSiO_2$ A and -B and the coatings (Dur-AgNPs-$nSiO_2$ A and -B) was tested through the zone of inhibition test according to the NCCLS M2-A9 standard test [52] using non-pathogenic strain of *Staphylococcus epidermidis* (Gram-positive, ATCC14990). For the powders, pellets with a diameter of 1.3 cm were made with 150 mg of the samples AgNPs-$nSiO_2$-A and -B by using a manual press by compacting the powders at 100 bar for 1 min; as a control a pellet was made with SiO_2 nanospheres synthesized as described previously without the addition of silver nitrate. *S. epidermidis* colonies were inoculated in Mueller–Hinton broth to obtain a bacterial suspension with a McFarland turbidity standard of 0.5 (1×10^8 CFU/mL), which was then uniformly spread onto Mueller–Hinton agar. The samples were placed in direct contact with the agar surface and incubated at 35 °C for 24 h. Antibacterial activity was assessed by observing the formation of a clear inhibition zone around the sample, indicating suppression of bacterial growth. The inhibition halo was

observed after 24h and 48 h of incubation and was measured quantitatively.

2.6. Leaching test in water

The release of silver ions from the coatings was evaluated using a leaching test in Milli-Q water at room temperature. Soda-lime glass samples (1×1 cm^2) with coated surfaces were placed face-up in 30 mL of water. The solutions were analyzed at regular intervals over a 24-h period using a spectrophotometer (Hanna Instruments) to quantify silver ion concentrations in parts per million (ppm). Each measurement was performed in triplicate to ensure accuracy.

3. Results and discussion

3.1. Morphological, compositional and structural characterization of $nSiO_2$-AgNPs powders

FESEM micrographs (Fig. 2) report the images relative to the AgNPs-$nSiO_2$ A and -B, obtained by means the two approaches A and B, compared with the silica nanospheres without silver. The powder of $nSiO_2$ was deposited onto carbon tape before the analysis in order to eliminate the charge effect on the electron micrographs. $nSiO_2$ (Fig. 2a and b) appeared spherical and with a diameter of 368.2 ± 9.6 nm for $nSiO_2$, 471.4 ± 29.8 nm for AgNPs-$nSiO_2$ A and 440.1 ± 25.6 for AgNPs-$nSiO_2$ B. No distinctions were evident between pure $nSiO_2$ and those functionalized at magnification of 10K (Fig. 2 a vs c and e). However, at higher magnification, the images show the presence of very small nanoparticles (<50 nm) displayed on the surface of the silica spheres attributable to the formation of silver nanoparticles (Fig. 2 d and f). In addition, the sample AgNPs-$nSiO_2$ B (f) revealed a greater presence of smaller nanoparticles on the surface of the silica nanospheres, suggesting a greater functionalization of silica nanospheres with silver nanoparticles compared to the ones obtained with the method A (Fig. 2 (d)).

To gain insight into the distribution and surface concentration of silver nanoparticles, as well as the differences resulting from the two synthesis approaches, high-resolution FESEM images were acquired after depositing the AgNPs-$nSiO_2$ powders onto TEM grids. As shown in Fig. 3, both samples exhibit small, bright nanoparticles on the surface of the silica spheres, which can be attributed to silver nanoparticles. Notably, the AgNPs-$nSiO_2$ A sample (Fig. 3a) shows fewer and smaller AgNPs, whereas the AgNPs-$nSiO_2$ B (Fig. 3b) sample features larger and more densely packed nanoparticles. The average diameter of AgNPs in sample A is 9.9 ± 2.9 nm, compared to 16.2 ± 3.2 nm in sample B.

EDS compositional analysis (Table 1) was conducted at a low magnification (500X), with the mean concentration value calculated across three distinct areas. The findings validated the presence of a higher silver content in sample AgNPs-$nSiO_2$-B confirming a higher presence of silver nanoparticles in the filler obtained with the method B. The slight variation in silver content between the two samples can be ascribed to the different solvent amounts used during the addition of the silver precursor. In previous sol–gel systems, lower solvent volumes favored ion adsorption on the particle surface due to reduced dilution [51]; however, in the present case, the higher solvent amount likely

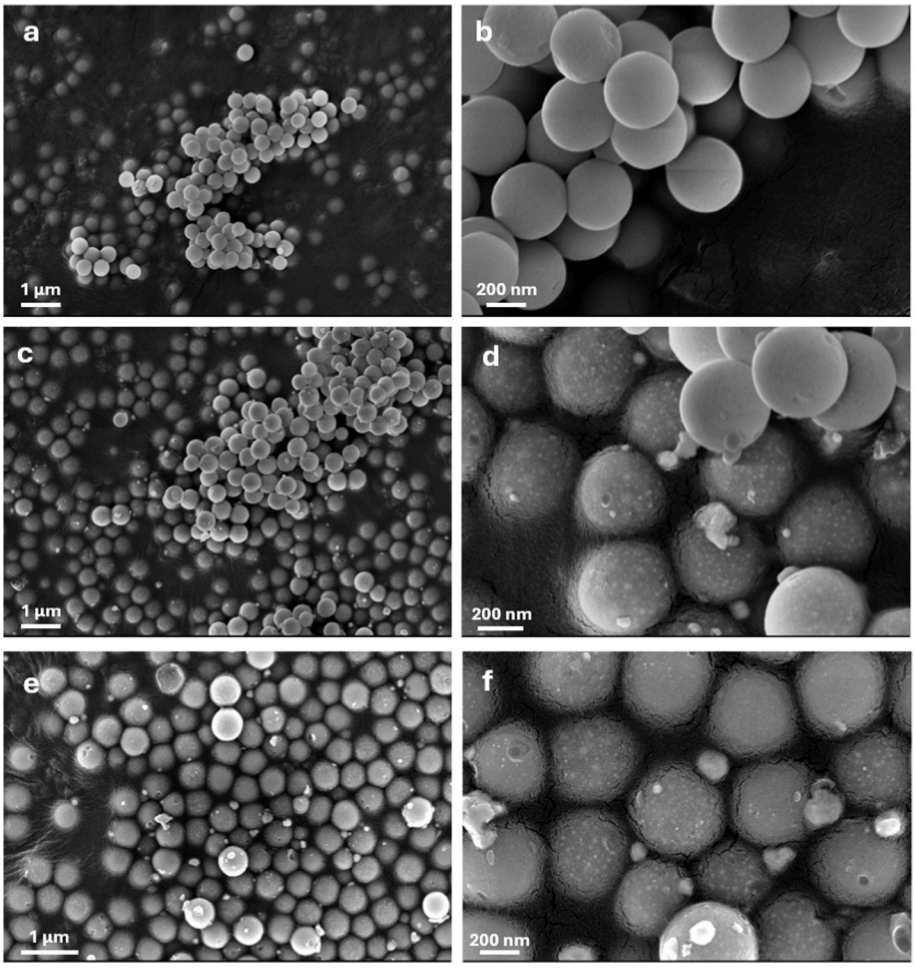

Fig. 2. FESEM images of the silica nanospheres (a, b) $nSiO_2$ and the silica nanospheres decorated with silver nanoparticles obtained from the two approaches: (c, d) AgNPs-$nSiO_2$ A and (e, f) AgNPs-$nSiO_2$ B.

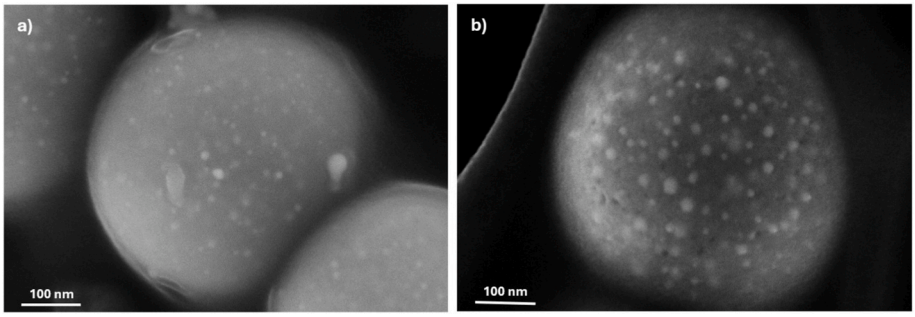

Fig. 3. High-resolution FESEM images of AgNPs-nSiO$_2$ A (a) and AgNPs-nSiO$_2$ B (b), captured at 150,000 × .

Table 1
Atomic percentage of the silicon and silver in the samples nSiO$_2$, AgNPs-nSiO$_2$-A and AgNPs-nSiO$_2$-B. Oxygen was also detected but is not reported in the table.

Powder	%atomic	
	Si	Ag
nSiO$_2$	34.1 ± 0.8	–
AgNPs-nSiO$_2$-A	32.0 ± 0.2	2.6 ± 0.3
AgNPs-nSiO$_2$ -B	31.1 ± 0.01	4.4 ± 0.02

improved the dissolution and dispersion of the silver salt, resulting in a more efficient incorporation of silver species. In addition, the simultaneous presence of residual TEOS in the synthesis of sample B may have further influenced silver nucleation and adsorption onto the silica surface.

In order to assess the presence of metallic silver on the silica nanospheres, the X-ray diffraction analysis was performed on the powders of AgNPs-nSiO$_2$ A and AgNPs-nSiO$_2$ B and the results were compared to the pattern obtained on the silica nanospheres nSiO$_2$. As shown in Fig. 4a, the patterns from all the samples show the broad halo located at 2θ between 20° and 30° that corresponds to the amorphous phase of the synthesized silica nanospheres [53]. In the pattern relative to the silver decorated silica nanospheres all the peaks associated with the crystalline structure of metallic silver (38.1°, 44.3°, 64.4°, 77.5° and 81.5°, Ag JCPDS code: 04–0783 [54]), were detected, indicating the successful reduction of silver ions into its metallic form during the heat treatment. By looking at the shape of the pattern peaks of silver, the peaks in the AgNPs-nSiO$_2$ -B appear more intense and narrow, suggesting that the amount of metallic silver on the surface of silica nanospheres is higher compared to the AgNPs-nSiO$_2$-A powder according to the EDS results and to the analysis of the morphological images [50]. In addition, the crystallite size of metallic silver was estimated by applying the Scherrer equation [55]; the resulting crystallite sizes were approximately 27 nm for the AgNPs–nSiO$_2$ A sample and 30 nm for the AgNPs–nSiO$_2$ B sample, confirming slightly larger crystalline domains in the latter. These values are in qualitative agreement with the FESEM observations, which revealed Ag nanoparticles with average diameters of ~10 nm and ~16 nm, respectively. The lower size values obtained from FESEM can be partly attributed to the intrinsic limitations of high-resolution imaging on insulating silica nanospheres.

FTIR analysis was conducted to identify the chemical groups present in the samples, with the results shown in Fig. 4b. In all three spectra, the most prominent peak appears at 1120 cm^{-1} and can be attributed to the asymmetric stretching vibration of Si–O–Si bonds. Additionally, the peak observed at 820 cm^{-1} corresponds to the symmetric stretching mode of the same Si–O–Si network [56]. In the nSiO$_2$ sample that did not undergo heat treatment, absorption bands associated with O–H and Si–OH groups are still evident. These signals are likely due to the presence of hydroxyl and silanol groups, which are commonly found in silica synthesized via the sol–precipitation method from tetraethyl orthosilicate (TEOS) [57].

3.2. Antibacterial effect of AgNPs-SiO$_2$ powder

The inhibition halo test (Fig. 5) was performed using a *Staphylococcus epidermidis* strain in order to evaluate the antibacterial activity of the silver decorated silica nanospheres, comparing the results with the silica nanospheres without silver. After 24 and 48 h of incubation, circular halo of 2.8 ± 0.7 mm and 3 ± 0.3 mm, respectively, were observed around the AgNPs-nSiO$_2$ A and AgNPs-nSiO$_2$ B, indicating antibacterial activity. In contrast, the control SiO$_2$ does not exhibit any antibacterial effect, permitting bacterial colonies to proliferate around it. The slightly larger inhibition zone observed for AgNPs–nSiO$_2$ B is consistent with its

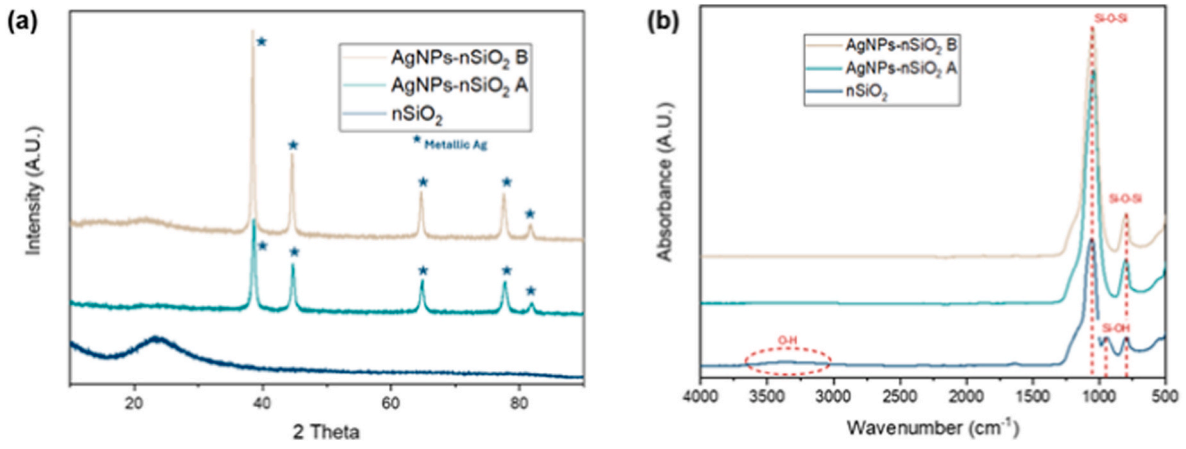

Fig. 4. XRD patterns of silica nanospheres without silver (nSiO$_2$) and Ag decorated silica nanospheres (AgNPs-nSiO$_2$ A and AgNPs-nSiO$_2$ B) (a). ATR-FTIR spectra of the samples nSiO$_2$, AgNPs-nSiO$_2$ A and AgNPs-nSiO$_2$ B (b).

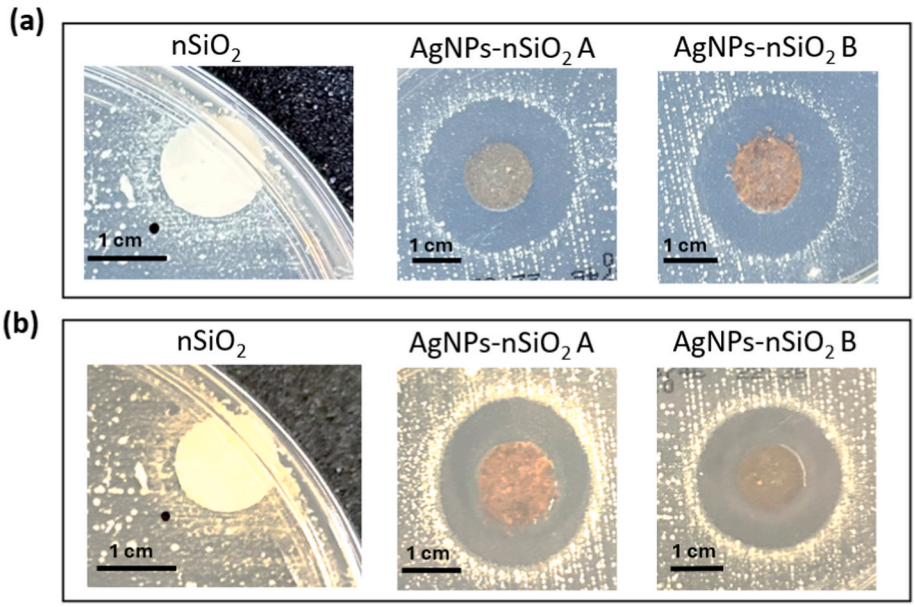

Fig. 5. Photos of the results of inhibition halo test against S. epidermidis relative to AgNPs-nSiO$_2$ A and -B compared with the control SiO$_2$ nanopowder, in the shape of pellets after (a) 24h and (b) 48h of incubation.

higher silver loading and with the higher density/larger size of AgNPs observed in this sample compared to AgNPs–nSiO$_2$ A (Figs. 3 and 4 and Table 1). This suggests that not only the presence of silver, but also its surface availability and distribution on the nanospheres, plays a role in the antibacterial response. The differences in synthesis conditions between the A and B routes translate into measurable differences in antibacterial performance.

3.3. Morphological, compositional and structural characterization of the Dur-AgNPs -nSiO$_2$ coatings

Fig. 6 shows FESEM images of the coatings containing silica nanospheres (nSiO$_2$) and silver-decorated silica nanospheres (AgNPs-nSiO$_2$) embedded in a polysilazane matrix. In all images, the large gray areas correspond to the continuous polysilazane matrix, which forms a dense, compact layer across the substrate surface.

In the control coating containing only silica nanospheres (Dur-nSiO$_2$, Fig. 5a), spherical nSiO$_2$ particles are homogeneously dispersed within the matrix and appear partially embedded or protruding from the polymer surface. No evidence of particle agglomeration is observed, which is a common issue during the synthesis of such doped coatings [27].

Coatings containing silver-decorated silica nanospheres (Dur-AgNPs-nSiO$_2$-A and -B, Fig. 5b and c) exhibit a similar morphology. The silica nanospheres are again well distributed within the matrix, confirming the suitability of nSiO$_2$ as a stable and uniform filler and effective carrier for silver nanoparticles. However, the FESEM micrographs also reveal that the nanospheres are consistently coated by the polysilazane matrix. This

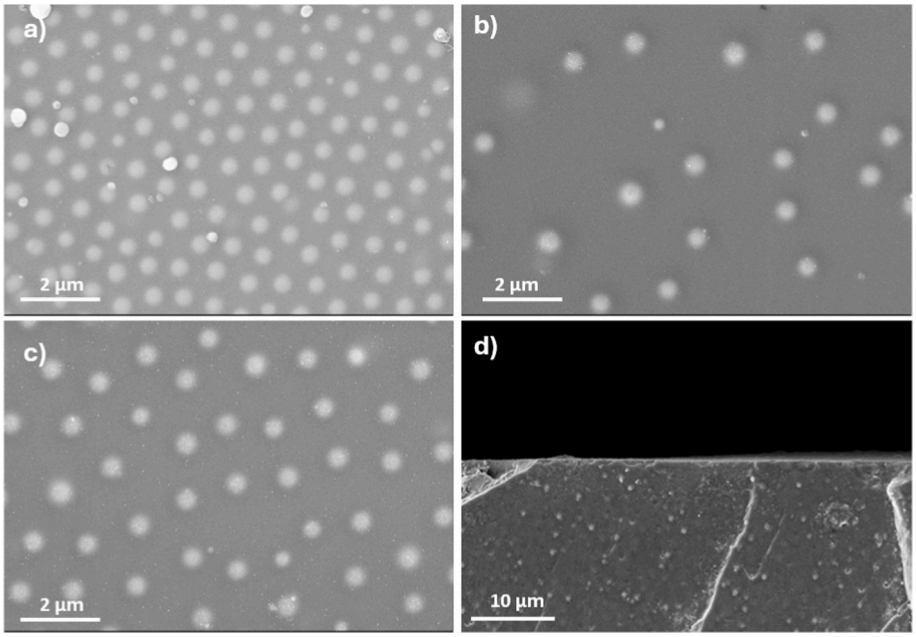

Fig. 6. Top-view FESEM images of the coatings (a) Dur-nSiO$_2$, (b) Dur-AgNPs-nSiO$_2$ A and (c) Dur-AgNPs-nSiO$_2$ B and cross-sectional FESEM images of the coating Dur-AgNPs-nSiO$_2$ B (d).

is evident from the smooth and continuous layer surrounding the particles and the lack of sharp interfacial contrast typically expected for bare particle surfaces.

At higher magnification (Figure SI 1), the silica nanospheres appear embedded within the matrix, with only their general shape protruding slightly. Even in the samples containing silver-decorated particles (Figure SI 1b, c), where small bright spots may be attributed to AgNPs, these features are located on particles that still appear partially encapsulated.

Overall, the coating structure appears dense and continuous, with no observable porosity or significant surface exposure of the fillers, factors that likely contribute to the limited antibacterial performance of the final composite.

To further investigate the internal morphology of the coating and confirm the distribution of the filler within the bulk, cross-sectional FESEM images of the Dur-AgNPs-nSiO_2 B sample were acquired and are reported in Fig. 6d and Figure SI 1d. As shown, the cross-section closely resembles the top-view morphology: the polysilazane matrix forms a dense and continuous phase, with no visible porosity or microcracks. The AgNPs-nSiO_2 B filler is homogeneously dispersed throughout the coating thickness, and no particles appear to protrude toward the surface. Importantly, even in cross-sectional view, the silica nanospheres are fully embedded within the matrix, and the silver nanoparticles remain unexposed (Figure SI 1d). This confirms that the encapsulation of the active phase persists throughout the entire coating volume, likely limiting both the direct contact of AgNPs with bacteria and the release of Ag^+ ions.

EDS analysis was performed on the two samples and the control Dur-nSiO_2 on an area at 5k of magnification an on the particles displayed in the coatings with a punctual analysis. Both samples show a low amount of silver in the coating (Table 2) but when a punctual EDS is performed on the smaller particles that are decorating the silica nanospheres, the atomic percentage of silver tends to increase as depicted in Table 2. In general, the sample Dur-AgNPs -nSiO_2 B shows a higher silver amount, according to the results of the EDS analysis on the silica powders.

The XRD patterns of the two coatings Dur-AgNPs-nSiO_2-A and Dur-AgNPs-nSiO_2-B were compared with the coating containing only silica nanospheres without silver (Dur-nSiO_2) (Fig. 7a). In all the tested samples, the amorphous structure of Durazane 1800 is recognizable by the halo between 20 and 30° [58]. While no peaks in the sample Dur-nSiO_2 are detected, both the functionalized coatings show the presence of the characteristic diffraction peaks of Ag^0, corresponding to the (111), (200), and (220) planes of the face-centered cubic (fcc) structure, are clearly visible, indicating that silver remains in its metallic state after incorporation [54] and confirming the successfully dispersion of the silver-decorated silica nanospheres in the polymeric matrix. By examining the shape of the metallic silver peaks in the Dur-AgNPs-nSiO_2-B sample, it is observed that the peaks are narrower and more intense according to the results obtained on the AgNPs-nSiO_2-A analysis in Fig. 3. This confirms that the intensity of the composite coating pattern peaks also increases with a higher concentration of silver [50] according to the EDS analysis.

FT-IR spectra were collected on the coatings after incorporation of the nanosilica into the polysilazane matrix and are reported in Fig. 7b. All three spectra are essentially identical, indicating that the chemical signature is dominated by Durazane 1800. Characteristic bands include C–H stretching at ≈ 2956 cm^{-1}, Si–H stretching at ≈ 2127 cm^{-1}, and Si–CH_3 bending at ≈ 1253 cm^{-1} [59]. With the exposure to air hydrolysis/condensation of the polysilazane backbone gives rise to a broad Si–O–Si asymmetric stretching band at ≈ 1060 cm^{-1}, while the N–H deformation (≈1180 cm^{-1}) and the Si–N–Si modes at ≈ 920 and 840 cm^{-1} disappear, consistent with Si–N to Si–O conversion [60,61].

Because all observed bands correspond to Durazane 1800, the spectra confirm that the silica nanospheres are completely coated by the polymeric matrix. This encapsulation is likely facilitated by residual surface –OH groups on the silica, which could enhance adhesion with the polysilazane [24].

Table 2
EDS atomic percentage of silicon and silver relative to the coatings Dur-nSiO_2, Dur-AgNPs-nSiO_2-A and Dur-AgNPs-nSiO_2-B considering areas and particle (punctual anaylsis). Carbon, oxygen and nitrogen were also detected but are not reported in the table.

Element	%atomic				
	Dur-nSiO_2	Dur-AgNPs-nSiO_2-A		Dur-AgNPs-nSiO_2-B	
	area	area	particle	area	particle
Si	37.3	32.6	34.0 ± 0.1	58.2	42.1 ± 0.6
Ag	–	**0.2**	**1.1 ± 0.2**	**0.4**	**1.65 ± 0.4**

3.4. Antibacterial efficacy of the Dur- AgNPs-nSiO_2 coatings

The antibacterial properties of the composite coatings were tested as for the fillers themselves with the inhibition halo test. However, after 24 and 48 h of incubation, no inhibition halo is visible around all the samples, including those containing silver nanoparticles as shown in Fig. 8. The results of the test show that the coatings have no antibacterial efficacy against the bacterium *S. epidermidis* contrarily to the silver-functionalized silica nanospheres themselves. This could be related to the very dense matrix in which the nanospheres have been encapsulated. In fact, the antibacterial efficacy of AgNPs primarily stems from two mechanisms: the release of Ag^+ and direct contact with bacterial cells. Ag^+ can disrupt vital cellular processes, while direct contact can lead to membrane damage and oxidative stress within bacteria [62]. In these coatings, the dense polysilazane matrix may impede both mechanisms. FESEM images suggest that AgNPs are embedded within the matrix, limiting their exposure to the surface. This encapsulation can reduce direct interactions with bacterial cells, thereby diminishing antibacterial activity.

Furthermore, the lack of porosity in the coating restricts the diffusion pathways necessary for Ag^+ to reach the external environment. Studies have shown that porous structures facilitate better ion release and enhance antibacterial performance [63].

3.5. Leaching test in water of the Dur- AgNPs-nSiO_2 coatings

Silver nanoparticles are known to release silver ions when in contact with water or, more generally, with aqueous environments [64]. To better understand the lack of antibacterial activity observed in the inhibition halo test, silver ion release from the coatings was evaluated, and the results are reported in Table 3. After 24 h, the concentration of released silver ions was found to be below the minimum inhibitory concentration (MIC) reported in the literature for several bacterial strains [65]. The release of Ag^+ ions from metallic silver nanoparticles is a surface-driven mechanism [66]; the intrinsic hydrophobic nature of the Durazane 1800 matrix, resulting from the exposure of –CH_3 groups, significantly limits water adsorption and penetration [67]. These chemical constraints are further compounded by structural factors.

The morphological analysis revealed that the polysilazane matrix forms a dense, non-porous layer that likely limits contact with the surrounding medium and hinders silver ion diffusion [68]. The low amount of silver detected is likely attributable to the limited number of nanoparticles partially exposed at the coating surface, with the highest release observed in the sample that also showed the highest silver content by EDS analysis.

4. Conclusions

This study aimed to synthesize silver nanoparticles decorated silica nanospheres and integrate them as a functional filler into the polymeric matrix of Durazane 1800, with the ultimate goal of enhancing

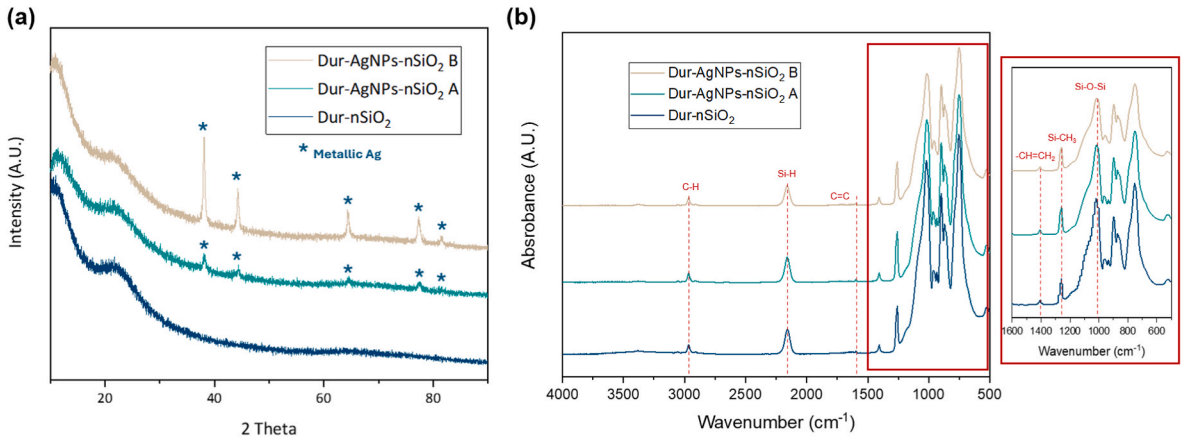

Fig. 7. XRD patterns of the coatings Dur-nSiO$_2$, Dur-AgNPs -nSiO$_2$-A, Dur-AgNPs -nSiO$_2$-B (a). ATR-FTIR spectra of the samples Dur-nSiO$_2$, Dur-AgNPs-nSiO$_2$ A and Dur-AgNPs-nSiO$_2$ B (b).

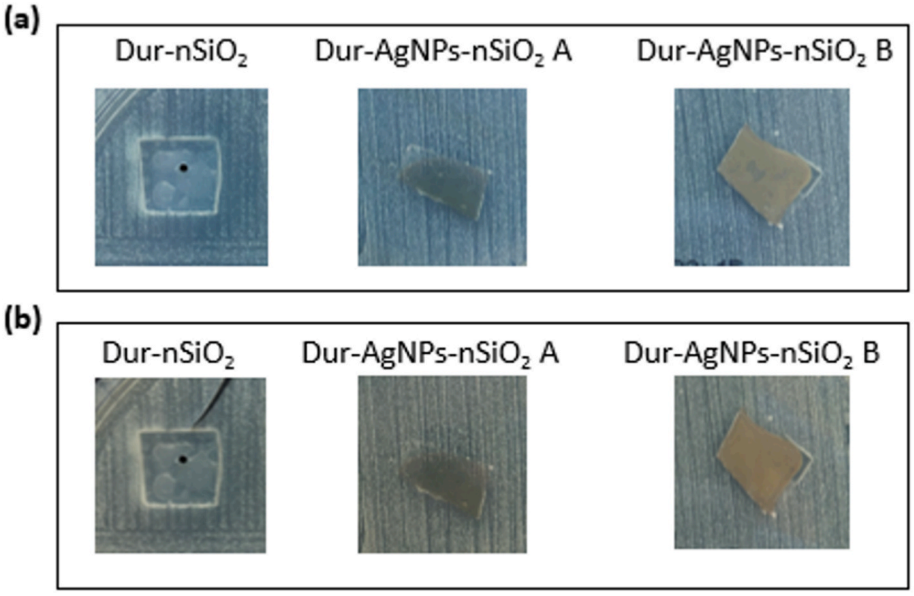

Fig. 8. Photos of the results of inhibition halo test against S. epidermidis with Dur-AgNPs-nSiO$_2$ A and Dur-AgNPs-nSiO$_2$ B compared with the control Dur-nSiO$_2$, after (a) 24h and (b) 48h of incubation.

Table 3
Amount of ionic silver released in water during silver leaching test in 24 h from the coated samples Dur- AgNPs-nSiO$_2$ A and B.

Sample	Ag^+ (ppm)
Dur-AgNPs-nSiO$_2$-A	0.016 ± 0.009
Dur-AgNPs-nSiO$_2$ -B	0.019 ± 0.007

antimicrobial efficacy. The successful synthesis of AgNPs-functionalized silica nanospheres with two different concentrations of silver nanoparticles demonstrated outstanding antibacterial efficacy. Subsequently, these nanoparticles were incorporated into the polymeric matrix of Durazane 1800. The homogeneous dispersion of the filler was confirmed throughout the coating, demonstrating the suitability of nSiO$_2$ as a carrier for the silver in the polysilazane matrix. This represents an initial phase towards achieving a composite coating with antibacterial attributes. Future research will focus on optimizing the coating design to increase porosity and improve the surface accessibility of the embedded silver nanoparticles. Possible strategies include impregnation or surface functionalization of preceramic or ceramic matrices with Ag-based species, as recently reported in the literature [69–71] as well as chemical or plasma etching treatments to enhance the exposure and antibacterial efficiency of the silver phase. The incorporation of sacrificial porogens that can be removed post-deposition also represents a promising approach to create micro- or nano-scale pathways for ion diffusion [72]. In addition, thermal treatment could modify the chemical nature of the polysilazane matrix by decomposing –CH$_3$ groups, thereby increasing its hydrophilicity and enabling water absorption and subsequent silver ion release. The ultimate goal of these efforts is to facilitate the controlled release of silver ions from the coating surface, thereby improving the antimicrobial performance of the material without compromising its structural integrity.

To improve reproducibility and control over film thickness and morphology, spin-coating deposition methods will be adopted in place of manual application in subsequent developments.

CRediT authorship contribution statement

Francesca Gattucci: Writing – review & editing, Writing – original draft, Visualization, Investigation. **Marta Miola:** Writing – review &

editing, Writing – original draft, Methodology, Investigation. **Cristina Balagna:** Writing – review & editing, Writing – original draft, Validation, Supervision, Resources, Project administration, Methodology, Investigation, Funding acquisition, Conceptualization.

Declaration of competing interest

The authors declare that they have no known competing financial interests or personal relationships that could have appeared to influence the work reported in this paper.

Acknowledgments

This study was carried out within the MICS (Made in Italy – Circular and Sustainable) Extended Partnership and received funding from the European Union Next-Generation EU (PIANO NAZIONALE DI RIPRESA E RESILIENZA (PNRR) – MISSIONE 4 COMPONENTE 2, INVESTIMENTO 1.3 – D.D. 1551.11-10-2022, PE00000004). This manuscript reflects only the authors' views and opinions, neither the European Union nor the European Commission can be considered responsible for them. The experimental activity of MSc Martina Tetti is kindly acknowledged.

Appendix A. Supplementary data

Supplementary data to this article can be found online at https://doi.org/10.1016/j.ceramint.2025.11.298.

References

[1] J.A. Lichter, K.J. Van Vliet, M.F. Rubner, Design of antibacterial surfaces and interfaces: polyelectrolyte multilayers as a multifunctional platform, Macromolecules 42 (2009) 8573–8586, https://doi.org/10.1021/ma901356s.
[2] B. Aslam, W. Wang, M.I. Arshad, M. Khurshid, S. Muzammil, M.H. Rasool, M. A. Nisar, R.F. Alvi, M.A. Aslam, M.U. Qamar, M.K.F. Salamat, Z. Baloch, Antibiotic resistance: a rundown of a global crisis, Infect. Drug Resist. 11 (2018) 1645–1658, https://doi.org/10.2147/IDR.S173867.
[3] European Commission reference: EU action on antimicrobial resistance, (n.d.). https://ec.europa.eu/health/antimicrobial-resistance/eu-action-on-antimicrobial-resistance_en (accessed July 15, 2021).
[4] W.M. Sweileh, Global research publications on irrational use of antimicrobials: call for more research to contain antimicrobial resistance, Glob. Health 17 (2021) 94, https://doi.org/10.1186/s12992-021-00754-9.
[5] W. DeFlorio, S. Liu, A.R. White, T.M. Taylor, L. Cisneros-Zevallos, Y. Min, E.M. A. Scholar, Recent developments in antimicrobial and antifouling coatings to reduce or prevent contamination and cross-contamination of food contact surfaces by bacteria, Compr. Rev. Food Sci. Food Saf. 20 (2021) 3093–3134, https://doi.org/10.1111/1541-4337.12750.
[6] C.M. Crisan, T. Mocan, M. Manolea, L.I. Lasca, F.-A. Tăbăran, L. Mocan, Review on silver nanoparticles as a novel class of antibacterial solutions, Appl. Sci. 11 (2021) 1120, https://doi.org/10.3390/app11031120.
[7] I.X. Yin, J. Zhang, I.S. Zhao, M.L. Mei, Q. Li, C.H. Chu, The antibacterial mechanism of silver nanoparticles and its application in dentistry, Int. J. Nanomed. 15 (2020) 2555–2562, https://doi.org/10.2147/IJN.S246764.
[8] C. Balagna, S. Perero, E. Percivalle, E.V. Nepita, M. Ferraris, Virucidal effect against coronavirus SARS-CoV-2 of a silver nanocluster/silica composite sputtered coating, Open Ceram 1 (2020) 100006, https://doi.org/10.1016/j.oceram.2020.100006.
[9] A. Luceri, R. Francese, D. Lembo, M. Ferraris, C. Balagna, Silver nanoparticles: review of antiviral properties, mechanism of action and applications, Microorganisms 11 (2023) 629, https://doi.org/10.3390/microorganisms11030629.
[10] L. Guo, W. Yuan, Z. Lu, C.M. Li, Polymer/nanosilver composite coatings for antibacterial applications, Colloids Surf. A Physicochem. Eng. Asp. 439 (2013) 69–83, https://doi.org/10.1016/j.colsurfa.2012.12.029.
[11] M. Ferraris, S. Perero, M. Miola, S. Ferraris, E. Verné, J. Morgiel, Silver nanocluster–silica composite coatings with antibacterial properties, Mater. Chem. Phys. 120 (2010) 123–126, https://doi.org/10.1016/j.matchemphys.2009.10.034.
[12] C. Balagna, S. Ferraris, S. Perero, M. Miola, F. Baino, A. Coggiola, D. Dolcino, A. Battiato, C. Manfredotti, E. Vittone, E. Vernè, M. Ferraris, Silver nanocluster/silica composite coatings obtained by sputtering for antibacterial applications, in: J. Njuguna (Ed.), Struct. Nanocomposites, Springer Berlin Heidelberg, Berlin, Heidelberg, 2013, pp. 225–247, https://doi.org/10.1007/978-3-642-40322-4_10.
[13] G. Schultes, M. Schmidt, M. Truar, D. Goettel, O. Freitag-Weber, U. Werner, Co-deposition of silver nanoclusters and sputtered alumina for sensor devices, Thin Solid Films 515 (2007) 7790–7797, https://doi.org/10.1016/j.tsf.2007.03.183.
[14] R. Govindaraj, R. Kesavamoorthy, R. Mythili, B. Viswanathan, The formation and characterization of silver clusters in zirconia, J. Appl. Phys. 90 (2001) 958–963, https://doi.org/10.1063/1.1382831.
[15] M. Carbone, D.T. Donia, G. Sabbatella, R. Antiochia, Silver nanoparticles in polymeric matrices for fresh food packaging, J. King Saud Univ. Sci. 28 (2016) 273–279, https://doi.org/10.1016/j.jksus.2016.05.004.
[16] C. Zanca, S. Carbone, B. Patella, F. Lopresti, G. Aiello, V. Brucato, F. Carfì Pavia, V. La Carrubba, R. Inguanta, Composite coatings of chitosan and silver nanoparticles obtained by galvanic deposition for orthopedic implants, Polymers 14 (2022) 3915, https://doi.org/10.3390/polym14183915.
[17] H. Palza, R. Quijada, K. Delgado, Antimicrobial polymer composites with copper micro- and nanoparticles: effect of particle size and polymer matrix, J. Bioact. Compat Polym. 30 (2015) 366–380, https://doi.org/10.1177/0883911515578870.
[18] S. Mallakpour, V. Behranvand, Nanocomposites based on biosafe nano ZnO and different polymeric matrixes for antibacterial, optical, thermal and mechanical applications, Eur. Polym. J. 84 (2016) 377–403, https://doi.org/10.1016/j.eurpolymj.2016.09.028.
[19] C. Damm, H. Münstedt, A. Rösch, The antimicrobial efficacy of polyamide 6/silver-nano- and microcomposites, Mater. Chem. Phys. 108 (2008) 61–66, https://doi.org/10.1016/j.matchemphys.2007.09.002.
[20] B. Gardelle, S. Duquesne, C. Vu, S. Bourbigot, Thermal degradation and fire performance of polysilazane-based coatings, Thermochim. Acta 519 (2011) 28–37, https://doi.org/10.1016/j.tca.2011.02.025.
[21] T. Coan, G.S. Barroso, R.A.F. Machado, F.S. De Souza, A. Spinelli, G. Motz, A novel organic-inorganic PMMA/polysilazane hybrid polymer for corrosion protection, Prog. Org. Coating 89 (2015) 220–230, https://doi.org/10.1016/j.porgcoat.2015.09.011.
[22] V. Bakumov, K. Gueinzius, C. Hermann, M. Schwarz, E. Kroke, Polysilazane-derived antibacterial silver–ceramic nanocomposites, J. Eur. Ceram. Soc. 27 (2007) 3287–3292, https://doi.org/10.1016/j.jeurceramsoc.2007.01.004.
[23] G. Barroso, T. Kraus, U. Degenhardt, M. Scheffler, G. Motz, Functional coatings based on preceramic polymers, Adv. Eng. Mater. 18 (2016) 746–753, https://doi.org/10.1002/adem.201500600.
[24] A. Chatterjee, S. Sen, D. Ramakanth, S. Singh, P.K. Maji, Unravelling polysilazanes: synthesis, structure-property insights and versatile coating applications, Adv. Colloid Interface Sci. 342 (2025) 103508, https://doi.org/10.1016/j.cis.2025.103508.
[25] G. Barroso, M. Döring, A. Horcher, A. Kienzle, G. Motz, Polysilazane-based coatings with anti-adherent properties for easy release of plastics and composites from metal molds, Adv. Mater. Interfac. 7 (2020) 1901952, https://doi.org/10.1002/admi.201901952.
[26] A.P. Kulkarni, K. Munechika, K.M. Noone, J.M. Smith, D.S. Ginger, Phase transfer of large anisotropic plasmon resonant silver nanoparticles from aqueous to organic solution, Langmuir 25 (2009) 7932–7939, https://doi.org/10.1021/la900600z.
[27] M. Jasiorski, A. Leszkiewicz, S. Brzeziński, G. Bugla-Płoskońska, G. Malinowska, B. Borak, I. Karbownik, A. Baszczuk, W. Stręk, W. Doroszkiewicz, Textile with silver silica spheres: its antimicrobial activity against Escherichia coli and Staphylococcus aureus, J. Sol. Gel Sci. Technol. 51 (2009) 330–334, https://doi.org/10.1007/s10971-009-1902-9.
[28] B. Tessema, G. Gonfa, S. Mekuria Hailegiorgis, G.A. Workneh, T. Getachew Tadesse, Synthesis and evaluation of the anti-bacterial effect of modified silica gel supported silver nanoparticles on E. coli and S. aureus, Results Chem. 7 (2024) 101471, https://doi.org/10.1016/j.rechem.2024.101471.
[29] L. Pérez-Gandarillas, D. Aragón, C. Manteca, M. Gonzalez-Barriuso, L. Soriano, A. Casas, A. Yedra, Highly hydrophobic organic coatings based on organopolysilazanes and silica nanoparticles: evaluation of environmental degradation, Coatings 13 (2023) 537, https://doi.org/10.3390/coatings13030537.
[30] M. Ferraris, A. Benelli, V. Casalegno, P. Shashkov, V.M. Sglavo, Joining and coating of plasma electrolytic oxidated aluminum using a silica preceramic polymer, Coatings 14 (2024) 757, https://doi.org/10.3390/coatings14060757.
[31] M. Günthner, A. Schütz, U. Glatzel, K. Wang, R.K. Bordia, O. Greißl, W. Krenkel, G. Motz, High performance environmental barrier coatings, part I: passive filler loaded SiCN system for steel, J. Eur. Ceram. Soc. 31 (2011) 3003–3010, https://doi.org/10.1016/j.jeurceramsoc.2011.05.027.
[32] I. Petríková, M. Parchovianský, P. Švančárek, M. Lenz Leite, G. Motz, D. Galusek, Passive filler loaded polysilazane-derived glass/ceramic coating system applied to AISI 441 stainless steel, part 1: processing and characterization, Int. J. Appl. Ceram. Technol. 17 (2020) 998–1009, https://doi.org/10.1111/ijac.13417.
[33] C.J. Chern, E. Beutler, Biochemical and electrophoretic studies of erythrocyte pyridoxine kinase in white and black Americans, Am. J. Hum. Genet. 28 (1976) 9–17.
[34] Q. Guo, P. Zhu, G. Li, L. Huang, Y. Zhang, D.D. Lu, R. Sun, C. Wong, One-pot synthesis of bimodal silica nanospheres and their effects on the rheological and thermal–mechanical properties of silica–epoxy composites, RSC Adv. 5 (2015) 50073–50081, https://doi.org/10.1039/C5RA06914A.
[35] M. Sangermano, G. Malucelli, E. Amerio, A. Priola, E. Billi, G. Rizza, Photopolymerization of epoxy coatings containing silica nanoparticles, Prog. Org. Coating 54 (2005) 134–138, https://doi.org/10.1016/j.porgcoat.2005.05.004.
[36] E. Amerio, P. Fabbri, G. Malucelli, M. Messori, M. Sangermano, R. Taurino, Scratch resistance of nano-silica reinforced acrylic coatings, Prog. Org. Coating 62 (2008) 129–133, https://doi.org/10.1016/j.porgcoat.2007.10.003.
[37] V. Volcanes Moreno, L. Yohai, R. Procaccini, S. Pellice, Silver-functionalized mesoporous silica nanoparticle coatings: optimal thermal stability and ionic activity for antimicrobial applications, Colloids Surf. A Physicochem. Eng. Asp. 711 (2025) 136387, https://doi.org/10.1016/j.colsurfa.2025.136387.

[38] J. Liu, S. Li, Y. Fang, Z. Zhu, Boosting antibacterial activity with mesoporous silica nanoparticles supported silver nanoclusters, J. Colloid Interface Sci. 555 (2019) 470–479, https://doi.org/10.1016/j.jcis.2019.08.009.
[39] S. Joardar, M.L. Adams, R. Biswas, G.V. Deodhar, K.E. Metzger, K. Deweese, M. Davidson, R.M. Richards, B.G. Trewyn, P. Biswas, Direct synthesis of silver nanoparticles modified spherical mesoporous silica as efficient antibacterial materials, Microporous Mesoporous Mater. 313 (2021) 110824, https://doi.org/10.1016/j.micromeso.2020.110824.
[40] J.-X. Wang, L.-X. Wen, Z.-H. Wang, J.-F. Chen, Immobilization of silver on hollow silica nanospheres and nanotubes and their antibacterial effects, Mater. Chem. Phys. 96 (2006) 90–97, https://doi.org/10.1016/j.matchemphys.2005.06.045.
[41] R. Lu, W. Zou, H. Du, J. Wang, S. Zhang, Antimicrobial activity of Ag nanoclusters encapsulated in porous silica nanospheres, Ceram. Int. 40 (2014) 3693–3698, https://doi.org/10.1016/j.ceramint.2013.09.055.
[42] L.P. Singh, S.K. Bhattacharyya, R. Kumar, G. Mishra, U. Sharma, G. Singh, S. Ahalawat, Sol-gel processing of silica nanoparticles and their applications, Adv. Colloid Interface Sci. 214 (2014) 17–37, https://doi.org/10.1016/j.cis.2014.10.007.
[43] M. Li, J.W.Y. Lam, F. Mahtab, S. Chen, W. Zhang, Y. Hong, J. Xiong, Q. Zheng, B. Z. Tang, Biotin-decorated fluorescent silica nanoparticles with aggregation-induced emission characteristics: fabrication, cytotoxicity and biological applications, J. Mater. Chem. B 1 (2013) 676–684, https://doi.org/10.1039/C2TB00155A.
[44] Y. Wang, A.V. Biradar, C.T. Duncan, T. Asefa, Silica nanosphere-supported shaped Pd nanoparticles encapsulated with nanoporous silica shell: efficient and recyclable nanocatalysts, J. Mater. Chem. 20 (2010) 7834, https://doi.org/10.1039/c0jm01093f.
[45] R.I. Ruvalcaba-Ontiveros, J.G. Murillo-Ramírez, J.A. Medina-Vázquez, A. R. Carrasco-Hernández, J.A. Duarte-Möller, H.E. Esparza-Ponce, Synthesis of gold decorated silica nanoparticles and their photothermal properties, Micron 166 (2023) 103415, https://doi.org/10.1016/j.micron.2023.103415.
[46] K.V. Arun Kumar, J. John, T.R. Sooraj, S.A. Raj, N.V. Unnikrishnan, N.B. Selvaraj, Surface plasmon response of silver nanoparticles doped silica synthesised via sol-gel route, Appl. Surf. Sci. 472 (2019) 40–45, https://doi.org/10.1016/j.apsusc.2018.05.178.
[47] G. De, A. Licciulli, C. Massaro, L. Tapfer, M. Catalano, G. Battaglin, C. Meneghini, P. Mazzoldi, Silver nanocrystals in silica by sol-gel processing, J. Non-Cryst. Solids 194 (1996) 225–234, https://doi.org/10.1016/0022-3093(91)00511-F.
[48] A. Liberman, N. Mendez, W.C. Trogler, A.C. Kummel, Synthesis and surface functionalization of silica nanoparticles for nanomedicine, Surf. Sci. Rep. 69 (2014) 132–158, https://doi.org/10.1016/j.surfrep.2014.07.001.
[49] C. Vichery, J.-M. Nedelec, Bioactive glass nanoparticles: from synthesis to materials design for biomedical applications, Materials 9 (2016) 288, https://doi.org/10.3390/ma9040288.
[50] M. Jasiorski, K. Łuszczyk, A. Baszczuk, Morphology and absorption properties control of silver nanoparticles deposited on two types of sol–gel spherical silica substrates, J. Alloys Compd. 588 (2014) 70–74, https://doi.org/10.1016/j.jallcom.2013.10.244.
[51] M. Miola, E. Piatti, P. Sartori, E. Verné, Sol-gel synthesis of spherical monodispersed bioactive glass nanoparticles co-doped with boron and copper, J. Non-Cryst. Solids 622 (2023) 122653, https://doi.org/10.1016/j.jnoncrysol.2023.122653.
[52] NCCLS M2-A9, Performance Standards for Antimicrobial Disk Susceptibility Tests, Approved Standard, ninth ed., NCCLS, Villanova, PA, 2003.
[53] R.S. Dubey, Y.B.R.D. Rajesh, M.A. More, Synthesis and characterization of SiO2 nanoparticles via sol-gel method for industrial applications, Mater. Today Proc. 2 (2015) 3575–3579, https://doi.org/10.1016/j.matpr.2015.07.098.
[54] B.K. Mehta, M. Chhajlani, B.D. Shrivastava, Green synthesis of silver nanoparticles and their characterization by XRD, J. Phys. Conf. Ser. 836 (2017) 012050, https://doi.org/10.1088/1742-6596/836/1/012050.
[55] A. Zielińska, E. Skwarek, A. Zaleska, M. Gazda, J. Hupka, Preparation of silver nanoparticles with controlled particle size, Procedia Chem. 1 (2009) 1560–1566, https://doi.org/10.1016/j.proche.2009.11.004.
[56] H. Helmiyati, R.P. Suci, Nanocomposite of cellulose-ZnO/SiO2 as catalyst biodiesel methyl ester from virgin coconut oil, in: AIP Conf. Proc., AIP Publishing, Depok, Indonesia, 2019, https://doi.org/10.1063/1.5132490.
[57] J.M. Kim, S.M. Chang, S.M. Kong, K.-S. Kim, J. Kim, W.-S. Kim, Control of hydroxyl group content in silica particle synthesized by the sol-precipitation process, Ceram. Int. 35 (2009) 1015–1019, https://doi.org/10.1016/j.ceramint.2008.04.011.
[58] R. Anand, B.B. Nayak, S.K. Behera, A novel TiO2–TiC–TiC0.3N0.7–C–SiCN multiphase ceramic nanocomposite from preceramic polymer pyrolysis, J. Inorg. Organomet. Polym. Mater. 32 (2022) 3546–3555, https://doi.org/10.1007/s10904-022-02359-0.
[59] M. Lenz Leite, A. Viard, D. Galusek, G. Motz, In situ generated β-Yb2Si2O7 containing coatings for steel protection in extreme combustion environments, Adv. Mater. Interfac. 8 (2021) 2100384, https://doi.org/10.1002/admi.202100384.
[60] Y. Zhan, R. Grottenmüller, W. Li, F. Javaid, R. Riedel, Evaluation of mechanical properties and hydrophobicity of room-temperature, moisture-curable polysilazane coatings, J. Appl. Polym. Sci. 138 (2021), https://doi.org/10.1002/app.50469.
[61] H. Kozuka, K. Nakajima, H. Uchiyama, Superior properties of silica thin films prepared from perhydropolysilazane solutions at room temperature in comparison with conventional alkoxide-derived silica gel films, ACS Appl. Mater. Interfaces 5 (2013) 8329–8336, https://doi.org/10.1021/am400845y.
[62] T.C. Dakal, A. Kumar, R.S. Majumdar, V. Yadav, Mechanistic basis of antimicrobial actions of silver nanoparticles, Front. Microbiol. 7 (2016), https://doi.org/10.3389/fmicb.2016.01831.
[63] B.B. Berking, L. Mallen-Huertas, S.J. Rijpkema, D.A. Wilson, Porous polymersomes as carriers for silver nanoparticles and nanoclusters: advantages of compartmentalization for antimicrobial usage, Biomacromolecules 24 (2023) 5905–5914, https://doi.org/10.1021/acs.biomac.3c00925.
[64] B. Tomšič, B. Simončič, B. Orel, L. Černe, P.F. Tavčer, M. Zorko, I. Jerman, A. Vilčnik, J. Kovač, Sol–gel coating of cellulose fibres with antimicrobial and repellent properties, J. Sol. Gel Sci. Technol. 47 (2008) 44–57, https://doi.org/10.1007/s10971-008-1732-1.
[65] L. Kvitek, A. Panacek, R. Prucek, J. Soukupova, M. Vanickova, M. Kolar, R. Zboril, Antibacterial activity and toxicity of silver – nanosilver versus ionic silver, J. Phys. Conf. Ser. 304 (2011) 012029, https://doi.org/10.1088/1742-6596/304/1/012029.
[66] Z. Adamczyk, M. Oćwieja, H. Mrowiec, S. Walas, D. Lupa, Oxidative dissolution of silver nanoparticles: a new theoretical approach, J. Colloid Interface Sci. 469 (2016) 355–364, https://doi.org/10.1016/j.jcis.2015.12.051.
[67] H.F. Giraldo Mejía, K. Herrera Seitz, M. Valdés, A. Uheida, R.A. Procaccini, S. A. Pellice, Antibacterial performance of hybrid nanocomposite coatings containing clay and silver nanoparticles, Colloids Surf. A Physicochem. Eng. Asp. 628 (2021) 127354, https://doi.org/10.1016/j.colsurfa.2021.127354.
[68] C. Dang, Y. Yin, M. Xu, J. Pu, Hydrophobic noncrystalline porous starch (NCPS): dispersed silver nanoparticle suspension as an antibacterial coating for packaging paper, Bioresources 13 (2017) 192–207, https://doi.org/10.15376/biores.13.1.192-207.
[69] C. Bhan, A.K. Golder, Utilizing bioinspired AgNPs as an antibacterial agent to enhance ceramic membrane performance, J. Environ. Chem. Eng. 11 (2023) 110283, https://doi.org/10.1016/j.jece.2023.110283.
[70] G.M. Shayo, E. Elimbinzi, C. Fabian, T.E. Kibona, G.N. Shao, Enhancing water quality at the point of use through fabrication of silver nanoparticles impregnated ceramic water filters, J. Indian Chem. Soc. 102 (2025) 101882, https://doi.org/10.1016/j.jics.2025.101882.
[71] M. Gajek, E. Stodolak-Zych, R. Cholewiński, R. Pacan, I. Puchyrska, P. Sacha, E. Kaniuk, R. Kurpanik, A. Rapacz-Kmita, Preparation and testing of the activity of antibacterial coatings on polished ceramic tiles obtained in industrial conditions, Ceram. Int. 51 (2025) 12480–12488, https://doi.org/10.1016/j.ceramint.2025.01.090.
[72] T. Konegger, L.F. Williams, R.K. Bordia, Planar, polysilazane-derived porous ceramic supports for membrane and catalysis applications, J. Am. Ceram. Soc. 98 (2015) 3047–3053, https://doi.org/10.1111/jace.13758.